HHS Public Access

Author manuscript

Cancer Res. Author manuscript; available in PMC 2022 October 15.

Published in final edited form as:

Cancer Res. 2022 April 15; 82(8): 1518–1533. doi:10.1158/0008-5472.CAN-21-1807.

Autocrine canonical Wnt signaling primes noncanonical signaling through ROR1 in metastatic castration-resistant prostate cancer

Fen Ma[1], **Seiji Arai**[1,2], **Keshan Wang**[1,3], **Carla Calagua**[1], **Amanda R. Yuan**[1], **Larysa Poluben**[1], **Zhongkai Gu**[1], **Joshua W. Russo**[1], **David J. Einstein**[1], **Huihui Ye**[1,4], **Meng Xiao He**[5,6,7], **Yu Liu**[8], **Eliezer Van Allen**[6,7], **Adam G. Sowalsky**[9], **Manoj K. Bhasin**[1,10], **Xin Yuan**[1], **Steven P. Balk**[1]

[1]Department of Medicine and Cancer Center, Beth Israel Deaconess Medical Center and Harvard Medical School; Boston, MA, 02215, USA

[2]Department of Urology, Gunma University Hospital; Maebashi, Gunma, Japan

[3]Department of Urology, Union Hospital, Tongji Medical College, Huazhong University of Science and Technology; Wuhan, Hubei 430022, P.R. China

[4]Department of Pathology, UCLA David Geffen School of Medicine; Los Angeles, CA 90095

[5]Harvard Graduate Program in Biophysics, Harvard Medical School; Boston, MA 02115, USA

[6]Department of Medical Oncology, Dana Farber Cancer Institute; Boston, MA 02115

[7]Broad Institute of Harvard and MIT; Cambridge, MA 02142, USA

[8]Program in System Biology, Department of Biochemistry and Molecular Pharmacology, University of Massachusetts Medical School; Worcester, MA 01605, USA

[9]Laboratory of Genitourinary Cancer Pathogenesis, National Cancer Institute, National Institutes of Health; Bethesda, MD 20892, USA

[10]Departments of Pediatrics and Biomedical Informatics, Emory School of Medicine; Atlanta, GA 30322, USA

Abstract

Wnt signaling driven by genomic alterations in genes including APC and CTNNB, which encodes β-catenin, have been implicated in prostate cancer (PC) development and progression to metastatic castration-resistant PC (mCRPC). However, nongenomic drivers and downstream effectors of Wnt signaling in PC and the therapeutic potential of targeting this pathway in PC have not been fully established. Here we analyzed Wnt/β-catenin signaling in PC and identified effectors distinct from those found in other tissues, including AHR and RUNX1, which are linked to stem cell maintenance, and ROR1, a noncanonical Wnt5a co-receptor. Wnt/β-catenin signaling-mediated

Corresponding Authors: Steven P. Balk, Beth Israel Deaconess Medical Center; 330 Brookline Avenue, Boston, MA, 02215; phone 617-735-2065; Fax 617-735-2060; sbalk@bidmc.harvard.edu; or Xin Yuan, Beth Israel Deaconess Medical Center, 330 Brookline Avenue, Boston, MA, 02215; phone 617-735-2066; Fax 617-735-2060; xyuan@bidmc.harvard.edu.

Conflict of interests: Authors declare that they have no competing interests.

increases in ROR1 enhanced noncanonical responses to Wnt5a. Regarding upstream drivers, APC genomic loss, but not its epigenetic downregulation commonly observed in PC, was strongly associated with Wnt/β-catenin pathway activation in clinical samples. Tumor cell upregulation of the Wnt transporter Wntless (WLS) was strongly associated with Wnt/β-catenin pathway activity in primary PC but also associated with both canonical and noncanonical Wnt signaling in mCRPC. Immunohistochemistry confirmed tumor cell WLS expression in primary PC and mCRPC, and patient-derived PC xenografts expressing WLS were responsive to treatment with Wnt synthesis inhibitor ECT-159. These findings reveal that Wnt/β-catenin signaling in PC drives stem cell maintenance and invasion and primes for noncanonical Wnt signaling through ROR1. They further show that autocrine Wnt production is a nongenomic driver of canonical and noncanonical Wnt signaling in PC, which can be targeted with Wnt synthesis inhibitors to suppress tumor growth.

Keywords

Wnt; β-catenin; prostate cancer; castration-resistant prostate cancer; ROR1

INTRODUCTION

Wnt/β-catenin signaling is required for prostate organogenesis, and accumulating evidence indicates that alterations in this pathway contribute to prostate cancer (PC) in at least a subset of cases (1). The frequency of these alterations appears to be higher in metastatic castration-resistant prostate cancer (mCRPC), with *APC* alterations being most common (2–6). Recent studies have further linked increased Wnt signaling to progression after treatment with androgen receptor (AR) signaling inhibitors including abiraterone and enzalutamide (ENZ) (6–10). In addition to genomic alterations, the *APC* gene is amongst the most commonly hypermethylated genes in PC, and this epigenetic APC downregulation is associated with higher grade and metastatic disease (11,12). Previous studies have also identified additional nongenomic mechanisms that may drive Wnt/β-catenin activity in PC (13–15).

Aberrant Wnt/β-catenin pathway activation has been linked to functions including cancer stem cell maintenance and invasion, but its functions in PC remain to be established. Transgenic expression of stable β-catenin in mouse prostate causes hyperplasia and squamous differentiation (16–18), and can drive to PC when combined with *PTEN* loss (19). In contrast, prostate-specific depletion of *Apc* results in adenocarcinomas with high penetrance, possibly reflecting more potent Wnt pathway activation or additional *APC* mechanisms of action (20). Studies from several groups also have shown that androgen receptor (AR) can interact with β-catenin (21). Conversely, a study in men with mCRPC found that circulating tumor cells with low AR signaling had high levels of noncanonical Wnt signaling that could be driven by WNT5a (22). Finally, prostate stromal cell production of WNT16b can contribute to resistance to DNA damaging agents (23).

Drugs that suppress Wnt signaling are in clinical trials, but identifying Wnt-dependent tumors that may be most responsive to these agents is a challenge. Expression of nuclear β-catenin is not a reliable indicator of Wnt signaling, and genes that are commonly associated

with Wnt pathway activation (such as *MYC* and *CCND1*) are also regulated by multiple other mechanisms. There are Wnt signaling gene sets generated from a variety of sources, including one generated in colorectal cancer (CRC) cells (24), but the relevance to PC has not been assessed. In this study, we have identified a gene set reflecting Wnt/β-catenin signaling in PC, and have exploited it to identify mechanisms that are driving this pathway and downstream effectors in primary PC and mCRPC.

MATERIALS AND METHODS

Establishment of cells with transient/stable RNAi or a Wnt reporter

VCaP and CWR22Rv1 cells were from ATCC and were maintained under conditions recommended by the provider. LAPC4 cells were from the Charles Sawyers lab and maintained in RPMI-1640 medium with 10% FBS. Cell lines were authenticated by short tandem repeat (STR) analysis (ATCC) and used within 20 passages, and were routinely tested for Mycoplasma (R&D Systems). CWR22Rv1 cells with doxycycline-regulated *APC* silencing shRNA (RV1_tet_shAPC) or shNTC (Non_Target_Control, RV1_tet_shNTC) were established using lentiviral infection of pLKO-tet-on system. Oligos used to form shRNAs are listed in Supplementary Materials. Transient APC or RNF43 knockdowns in VCaP cells were performed as described previously (14). siRNAs used in this study are listed in Supplementary Materials. RNA or protein was extracted at 72 hours after transfection. CWR22-R1 is a PC cell line derived from CWR22 xenografts (25,26). R1-7TFP cell line used in this study was established by lentiviral transduction with a β-catenin/TCF-regulated luciferase reporter gene (Plasmid #24308, Addgene).

Quantitative reverse transcription PCR (RT-qPCR)

Total RNA was isolated using the RNeasy Mini Plus Kit (Qiagen). RT-qPCR used SYBR Green reagents from the StepOnePlus Real-Time PCR system (Thermo Fisher Scientific) or TaqMan One-Step RT-PCR reagents (Thermo Fisher Scientific). Target mRNA expression was quantified using the ΔΔCt method and normalized to GAPDH expression. Primer sequences and probe information are in Supplementary Materials.

RNA Sequencing Data Generation and Analysis

RNA-seq was performed on two biological replicates after 72 hours of knockdown with the following conditions in VCaP cells: SiNTC (non-target-control), SiAPC-2/3, SiRNF43-3/4, SiRNF43-3/4 plus Wnt3a (100 ng/ml for 7 hrs before harvesting the cells). Details on the RNA-seq and analysis are in Supplementary Materials. The GEO accession number for RNA-seq data generated in this study is GSE188557.

Pathway analysis

Metacore pathway analysis (Clarivate Analytics, RRID:SCR_008653) was used to assess the differentially regulated genes in VCaP with APC knockdown or RNF43 knockdown plus Wnt3a stimulation. Pathways enrichment was performed for commonly regulated genes as well as uniquely regulated genes in APC knockdown or RNF43 knockdown plus Wnt3a stimulation conditions. Ingenuity Pathway Analysis (IPA 9.0, Qiagen, RRID:SCR_008653) was also applied to interrogate the pathways and interaction networks enriched in

significantly differentially regulated genes in common. In addition, an upstream prediction analysis was performed for the significantly differentially regulated genes in common. A p-value for each pathway was generated according to the fit of input gene sets to the corresponding database using a one-tailed Fisher exact test. The pathways with p-values <0.05 were considered significantly affected.

Gene Set Enrichment Analysis (GSEA) and single-sample GSEA (ssGSEA)

We used several WNT gene sets to assess WNT activity for each patient in TCGA, SU2C, WCPCDT, and FHCRC datasets. We utilized a CRC-derived WNT signature (24), the KEGG WNT signature (KEGG,RRID:SCR_012773), and the BIOCARTA WNT signatures. WNT Pathway activity scores were calculated using the ssGSEA method (https://www.genepattern.org/modules/docs/ssGSEAProjection/). To interrogate the unique pathways regulated by APC in mCRPC samples, we selected cases with APC alterations, or WNT activity scores more than 5000 (presumably with APC methylation), which were classified as WNT activated samples in both SU2C and FHCRC datasets. We performed gene set enrichment analysis using the GSEA tool developed by the Broad Institute (https://www.gsea-msigdb.org/gsea/index.jsp) (SeqGSEA, RRID:SCR_006020). Candidate gene sets include all members of the “hallmark gene sets” and “canonical pathways” from the GSEA MSigDB database (version 7). To ensure that we only considered genes expressed at reasonable levels in multiple samples, we only included genes with a TPM value of greater than 1 in all samples. We then ranked genes from highest confidence enrichment in WNT activated samples to highest confidence enrichment in the rest of the samples, which serves as the input of the GSEAPreranked tool for pathway analysis, with a permutation of 1,000.

Wnt driver prediction

Samples from the TCGA dataset were stratified into Wnt high and low groups based on Wnt activity score generated from the Wnt47 gene signature. The top and bottom quartiles were selected and gene expression was compared between two groups and log2 transformed fold change was calculated. A differential expression gene list was generated with an adjusted P <0.05. We then filtered the list with curated Wnt component genes based on the WNT homepage developed by the Nusse lab (http://web.stanford.edu/group/nusselab/cgi-bin/wnt/) (Wnt Database, RRID:SCR_006020). Based on our previous study, SOX9 was also included in the list. To select the genes abundantly expressed in patients, only genes with positive average expression values were considered as potential drivers (highlighted in Fig. S5a). The curated WNT component gene list used for analysis is in Supplemental Materials.

Random Forest Analysis

Random Forest analysis was performed to predict the most significant downstream effectors of canonical WNT signaling in prostate cancer. The phenotype was defined based on WNT activity status. In VCaP cells, the WNT high versus WNT low groups were classified as APC knockdown or RNF43 knockdown plus Wnt3a stimulation versus controls. In TCGA datasets, samples with top quartile WNT activity scores were binned into the WNT high group, and the samples with bottom quartile WNT activity scores were binned into the WNT low group. We then addressed which genes were most essential for the classification.

The mean decrease in accuracy was used as measurement of importance in Random Forest analysis, and lists of most informative genes for classifying the WNT high versus WNT low groups were generated for both VCaP and TCGA datasets. A multidimensional scaling (MDS) plot was generated by intersecting important genes contributing to WNT activation in the TCGA dataset and VCaP cells with either APC knockdown or RNF43 knockdown plus Wnt3a stimulation. Genes that fall in the upper right quadrant are the most significant contributors.

Matrix Similarity Analysis

Matrix Similarity Analysis was performed to predict functional hubs for the WNT47 signature using Morpheus matrix visualization and analysis software developed by the Broad Institute. Log2 Fold Change (Log2FC) data of the WNT47 signature gene was used as the feed data. In VCaP cells, log2FC of each gene was calculated by comparing APC knockdown or RNF43 knockdown plus Wnt3a stimulation with controls. In clinical samples, the Log2FC of each gene was calculated by comparing samples with top quartile WNT activity scores and samples with bottom quartile WNT activity scores in each data set.

Survival Analysis

To compare outcomes in patients with high vs. low expression of *APC* gene (presumably through *APC* methylation), Kaplan Meier survival analysis was conducted through the c-Bioportal with log-rank testing for significance. Two datasets with disease-free survival information, including TCGA and MSKCC (Memorial Sloan Kettering Cancer Center), were selected for analysis. First, the expression profile of APC was assessed in each dataset. In the TCGA dataset, the criteria of sample selection were set as such APC: EXP>0.7 EXP<−0.7 that most approximate group size could be achieved for both APC high (62) and APC low (86) groups. Similarly, APC: EXP>0.7 EXP<−1.7 were applied to get a comparable group size for both APC high (12) and APC low (11) groups in the MSKCC dataset. Survival analysis was then performed based on APC expression in the defined samples. The altered group is APC low, whereas the unaltered group represents APC high.

CellTiter-Glo Luminescent Cell Viability Assay

RV1_tet_shAPC cells were cultured with or without doxycycline (400ng/ml) in 96 well plates. Cells were treated with four doses of pan PLK inhibitor (BI2563) and six doses of PLK1 inhibitor (PCM075), ranging from 2 to 10uM. Triplicates were set up for each dose. CellTiter-Glo luminescent cell viability assay (Promega, G7571) was performed after three days of treatment according to the manufacturer's protocol. The killing curve was plotted based on the readout (Fig. S4C). All experiments were repeated at least three times, and representative results were shown.

Immunoblotting and immunohistochemistry (IHC)

Immunoblotting and IHC experiments were performed as described before (14). Gels shown are representative of at least three independent experiments. For immunoblotting, proteins were extracted using RIPA buffer, and primary antibodies were incubated overnight. For IHC, 5-μm formalin-fixed, paraffin-embedded (FFPE) sections underwent epitope retrieval

using the Dako PT Link platform. Staining was on the Dako Link 48 autostainer, with amplification using EnVision FLEX mouse linkers, and visualization using the EnVision FLEX high-sensitivity visualization system (Dako). For WLS, sections were stained with an anti-WLS antibody YJ5 (Biolegand; 1:200). The mCRPC TMA in figure 4 contains 20 cases from the University of Washington rapid autopsy program. PORCN staining was similarly performed with anti-PORCN antibody (ab105543, Abcam, 1:200, RRID:AB_10860951). Primary antibodies are detailed in Supplemental Materials.

Xenografts and drug treatment

Male 5–6 week old ICR SCID mice (intact or castrated) were purchased from Taconic and housed in the Animal Research Facility at Beth Israel Deaconess Medical Center (BIDMC, Boston, MA). All procedures were approved by the BIDMC IACUC and conformed to NIH guidelines. For all xenograft studies, after tumors were established, mice were randomly assigned to experimental groups. For RV1 tumor growth studies, 5–6 weeks old ICR SCID mice were injected subcutaneously with one million of either RV1_tet_shAPC or RV1_tet_shNTC cells in 50% Matrigel. Five mice were inoculated for each group, and mice were fed with doxycycline chow (0.625 g/kg, Harlan Tekland) and water (1 mg/ml in 1% dextrose), commencing at the initial implantation. Once tumors were established (tumor volume, 100–200 mm^3), tumor sizes were followed twice a week by directly measuring with calipers.

For drug treatment studies in the R1-7TFP model, 5–6 week old ICR SCID mice (castrated) were injected subcutaneously with one million R1-7TFP PC cells. When tumors reached approximately 200 mm^3, the host was randomly assigned to the control or to treatment with the PORCN inhibitor ETC-1922159 (ETC-159, which is currently being evaluated in a phase 1 clinical trial, NCT02521844). For drug treatment studies in BIDPC5, LuCaP70CR and LuCaP77CR, 5–6 weeks old ICR SCID mice (castrated) were similarly injected subcutaneously with the respective patient derived xenograft (PDX). When tumors reached approximately 200 mm^3, the host was randomly assigned to the control or treatment groups. Tumor sizes were followed twice a week by directly measuring with a caliper. Fold changes of the tumor volume were calculated by normalizing each tumor to its size measured on day 1 (treatment starting point). The ETC-159 was kindly provided by A*STAR, Singapore. ENZ was purchased from Selleckchem.com. The treatment group received 30 mg/kg of ETC-159 (in 0.2 ml 0.5% carboxyl methyl-cellulose by oral gavage) every other day. The control group received the carrier solution only. ENZ was added to the drinking water to achieve a dose of 25 mg/kg/d.

ChIP-seq analysis

ChIP-seq data for TCF7L2 was obtained from LNCaP (GSM1249449) and HCT116 (GSM782123). H3K27Ac ChIP-seq data resources: LNCaP (GSM1902615), VCaP (GSM2537221), SW480 (GSM2058027), HT29 (GSM2042876) and HCT116 (GSM1890730). ChIP-seq profiles of TCF7L2 and H3K27Ac flanking the ROR1 gene were demonstrated using IGV reference to Hg38.

Statistics

GraphPad Prism 9 Software (GraphPad Software Inc., RRID:SCR_002798) was used for all statistical analysis unless otherwise specified. The significance of the difference between the two groups was determined by the 2-tailed Student's *t*-test. To assess the growth difference in the treatment studies, Mann-Whitney tests were used to compare the control versus ETC treatment groups. Pearson Correlation was used for all correlation analyses. The Log-rank test was used for survival analysis. Statistical significance was accepted at $P < 0.05$.

Data Availability Statement

The GEO accession number for RNA-seq data generated in this study is GSE188557.

RESULTS

Identification of Wnt/β-catenin signaling signature by transcriptome profiling in PC cells

Genomic alterations predicted to activate WNT/β-catenin signaling have been identified in ~10–26% of PC (Supplementary Fig. S1A, Supplementary Table S1). However, downstream effectors of this pathway in PC, and the activity of this pathway in tumors without these genomic alterations, remain unclear. We initially found that available Wnt/β-catenin pathway signatures could not clearly identify PC with loss of *APC* or stabilizing mutations in *CTNNB1* (Supplementary Fig. S1B). Therefore, we undertook to assess the response to physiological stimulation of this pathway in PC cells with WNT3a in conjunction with depletion of RNF43 or ZNRF3, the ubiquitin ligases that negatively regulate Wnt signaling.

Examination of the CCLE database showed that RNF43 and ZNRF3 were expressed at comparable levels across a panel of PC cells lines (Supplementary Fig. S1C), but knockdown of RNF43 or ZNRF3 did not enhance the responses to WNT3a in LNCaP, RV1, or PC3 cells (using AXIN2 as a measure of Wnt/β-catenin signaling) (Supplementary Fig. S1D). In VCaP cells, knockdown of RNF43, but not ZNRF3, potentiated the response to WNT3a (Supplementary Fig. S1E, F). Therefore, we carried out RNA-seq in VCaP cells depleted of RNF43 by siRNA and then stimulated with WNT3a, which altered the expression of 340 genes (P<0.05, Fig. 1A).

In parallel we assessed effects of *APC* depletion, which was comparably expressed among PC cell lines (Supplementary Fig. S1G). Treatment with 3 independent *APC* siRNA increased *AXIN2* expression to a much greater degree than WNT3a (Supplementary Fig. S1H), which may reflect APC suppression of nuclear β-catenin activity as well as its role in the cytoplasmic destruction complex (27). VCaP cells depleted of APC by 2 different siRNA caused the differential expression of 2436 genes (P<0.05, Fig. 1B). The greater number of genes affected by APC depletion may reflect both increased Wnt/β-catenin pathway activation and additional β-catenin independent activities of APC (28).

To enrich for direct downstream targets of WNT/β-catenin signaling, we intersected the two datasets to obtain a common 124-gene set (Fig. 1C). The top enriched pathways for these genes were Wnt signaling and several developmental pathways, all consistent with Wnt signaling (Fig. 1D). These associations were significantly greater for the common 124-gene

set than for the genes uniquely altered by either APC or RNF43/WNT3a, consistent with this gene set being more specific for Wnt/β-catenin signaling. In contrast, the gene sets uniquely altered by APC depletion were associated with cell cycle and cytoskeleton-related processes (Fig. 1E). Notably, previous studies have indicated that APC has Wnt pathway-independent functions related to these processes (27,29).

Refinement of Wnt/β-catenin signature by integration with clinical datasets

To assess the clinical relevance of these 124 genes and refine the WNT/β-catenin signature, we obtained the gene expression data from PC clinical datasets including TCGA (primary PC), Stand Up to Cancer (SU2C) and West Coast Prostate Cancer Dream Teams (WCPCDT) (mCRPC biopsies), and FHCRC (rapid autopsy samples) (1–3,30). Tumors in each dataset were ranked for Wnt/β-catenin pathway activity based on the 124-gene signature. A 47-gene subset of the 124 genes was then selected based on their association with Wnt signaling-high status in at least three of the datasets (Fig. 2A), which showed only minimal overlap with previously reported Wnt/β-catenin gene-sets (Supplementary Table S2). The top biological processes associated with these 47 genes were related to Wnt signaling (Fig. 2B–D). Notably, “negative regulators of Wnt signaling” was one of the prominent GO terms (Fig. 2B), consistent with increased Wnt signaling as these negative regulators (including AXIN2, GREM2, NKD1, and ZNRF3) are strongly induced by Wnt signaling.

Wnt activity scores based on the 47-gene signature were then generated for each tumor in the clinical datasets, which revealed a continuum of Wnt activty in both primary and metastatic PC (Supplementary Fig. S2). Notably, while tumors with *APC* loss had comparable high Wnt activity scores in each dataset (with more modest increases in the *CTNNB1*-mutant tumors), the mCRPC groups had lower Wnt activity scores in cases without *APC* or *CTNNB1* alterations (Fig. 2E–H). The LuCaP series of PC patient-derived xenografts (PDXs) also showed markedly higher Wnt activity scores in the tumors with *APC* losses (Fig. 2I). This range of Wnt activity in tumors without Wnt-related genomic alterations indicates that Wnt activity in these tumors may be driven by nongenomic mechanisms.

Epigenetic downregulation of APC is not associated with Wnt/β-catenin signaling

As noted above, *APC* loss was strongly associated with Wnt/β-catenin pathway activity. Interestingly, deep deletions of *APC* appear more common in primary PC, versus truncating mutations in mCRPC (Supplementary Fig. S3A). Similar to *APC* alterations in CRC, truncating mutations are clustered in the β-catenin interacting region, and in at least a subset of cases are associated with loss of the second copy (Supplementary Fig. S3B). The prevalence of these truncating mutations in CRC is presumed to reflect a requirement for some residual APC activity, and may confer responsiveness to tankyrase inhibitors (31). The more frequent genomic loss via deletion in primary PC indicates that such residual activity may be more important for metastatic growth.

APC is amongst the most highly methylated genes in PC (11,12), and this is associated with decreased mRNA (Fig. 3A), although effects on protein remain to be established. Survival analysis in the TCGA and MSKCC datasets show a trend of decreased disease-free

survival with reduced APC expression (Fig. 3B), suggesting that epigenetic downregulation of APC may confer a more aggressive phenotype. Interestingly, acute downregulation of APC by siRNA (~80% reduction), which markedly induced Wnt signaling, suppressed cell proliferation (Supplementary Fig. S4A) (28). In contrast, stably expressing an APC shRNA had only ~50% reduction, which is in the range of reduction seen *in vivo* due to increased methylation (Fig. 3A), and did not have impaired proliferation (Supplementary Fig. S4B). Therefore, we generated subcutaneous xenografts from these cells expressing APC shRNA versus control RV1 cells expressing a nontargeting shRNA. Consistent with a more aggressive phenotype, the APC knockdown xenografts developed earlier and grew more rapidly (Fig. 3C). Analysis of individual xenografts confirmed that APC mRNA was reduced to ~50% of control levels, and also showed a variable ~2–5-fold increase in AXIN2 (Fig. 3C).

These results indicated that enhanced tumor growth after downregulation of APC mRNA (and presumably APC protein, but reliable antibodies to assess this are not available) may reflect increases in Wnt/β-catenin pathway activation. However, analysis of the TCGA primary PC dataset showed that APC mRNA expression was positively, rather than negatively, correlated with Wnt/β-catenin pathway activity (Fig. 3D). Similarly, there was not a consistent inverse correlation in the mCRPC data sets (Fig. 3D). These findings indicate that the epigenetic downregulation of APC in PC *in vivo* does not activate Wnt/β-catenin signaling, and suggest this APC downregulation may be oncogenic through distinct Wnt/β-catenin-independent mechanisms. As noted in figure 1, gene sets related to mitosis were strongly associated with APC downregulation, but not with WNT3a stimulation. This is consistent with studies indicating a mitotic spindle scaffold function for APC (28), but oncogenic effects of loss of this function are unclear.

To further explore alternative oncogenic mechanisms, we integrated the cell cycle genes associated with APC depletion (but not with WNT3a stimulation) in VCaP cells and associated with high Wnt/β-catenin signaling in mCRPC (as these are predominantly APC-deficient) (Supplementary Table S3). We then further tested for association with APC expression, which yielded four genes (*CDK6*, *PLK1*, *BUB1* and *CDC25C*) that were inversely correlated with APC mRNA in mCRPC datasets (Fig. 3E). RT-qPCR confirmed the induction of these genes by APC siRNA (Supplementary Fig. S5A). One interpretation of these results is that APC downregulation is driving cells through cell cycle and thereby increasing expression of these genes. Alternatively, if APC downregulation has deleterious effects on the mitotic spindle, then these increases may be compensatory and reflect an increased dependence on PLK1, BUB1, and CDC25C. In support of the latter hypothesis, we found that APC downregulation *in vitro* enhanced sensitivity to a pan-PLK inhibitor (BI2536) and a PLK1-specific inhibitor (PCM075), although the differences were modest (Supplementary Fig. S5B). Overall these results indicate that epigenetic downregulation of APC is not driving Wnt/β-catenin signaling, but may contribute to aggressive behavior by distinct mechanisms.

Non-genomic mechanisms mediating Wnt pathway activation in clinical samples

Importantly, the initial 124-gene and the subsequently derived 47-gene set reflect downstream responses to Wnt pathway activation, but not upstream activators. To identify nongenomic upstream activators in primary PC, we stratified TCGA primary PC tumors into Wnt-signature-high and -low quartiles, and obtained 3356 genes that were differentially expressed between the two groups (absolute fold change >1.5 at $p<0.05$). We then filtered this list for all Wnt pathway related genes (Supplementary Table S4). Two genes on this filtered list are established downstream targets of Wnt signaling (*AXIN2* and *LEF1*), and 7 (in addition to *AXIN2*) are negative regulators of Wnt signaling (*DKK1-4*, *SFRP1,2,5*). The remaining genes expressed at substantial levels were *WLS* (Wntless, a ligand transporter required for Wnt production), *WNT2B*, *FZD1/3/7, LRP6*, *RSPO3*, *TCF7L2*, and SOX9 (Figure 4A).

The association of WLS mRNA with Wnt signaling was found in groups of samples with both low or high cellularity, indicating this association was not just a reflection of tumor content (Supplementary Fig. S6A). The WLS association with Wnt signaling indicated that tumor cell autocrine Wnt synthesis, or potentially paracrine Wnt synthesis by adjacent stromal cells, might be driving Wnt pathway activity. To investigate the source of Wnt, we performed immunohistochemistry for WLS. The specificity of the WLS antibody was first confirmed using cell blocks with WLS knockdown (Supplementary Fig. S6B). Staining of human prostate revealed WLS expression in basal epithelium, but not luminal epithelium, of normal glands (Figure 4B, **upper left panel**). There was a similar pattern in Prostatic Intraepithelial Neoplasia (PIN) lesions, with WLS in the discontinuous basal cell layer and minimal staining in the luminal cells (Figure 4B, **upper right panel**). These findings indicate that basal cells are the primary source of Wnts in normal prostate. In contrast, WLS in tumor foci was expressed primarily in tumor cells (Figure 4B, **upper right and bottom panels**), although we also observed scattered and variable staining in the surrounding stroma in some cases. WLS expression was also heterogeneous in some tumors (Figure 4B, **bottom right panel**). Overall these observations indicate that tumors acquire the capacity to produce Wnts.

The enzyme mediating Wnt palmitoylation (PORCN), was also correlated with Wnt activity in TCGA, although more weakly (Supplementary Fig. S6C). IHC showed PORCN expression in PC cells (Supplementary Fig. S6D), further supporting autocrine Wnt synthesis in primary PC. In contrast to primary PC, WLS mRNA expression was more weakly associated with Wnt/β-catenin signaling in mCRPC (Figure 4C). Nonetheless, WLS mRNA levels in primary PC and mCRPC were comparable, and by IHC we observed intermediate to high WLS expression in ~70% of mCRPC cases (Figure 4D), suggesting WLS may be driving more noncanonical Wnt signaling in mCRPC.

Downstream effectors of Wnt/β-catenin signaling in PC mediate diverse functions

Many of the genes in the 47-gene Wnt signature for PC are known negative regulators of Wnt signaling. Additional genes in common with other Wnt signatures were *LEF1* and *CD44*. Analyses for biological processes associated with these 47 genes did not suggest any further specific functions. Therefore, we next used Random Forest Analysis to identify the

subset of genes that were most associated with Wnt pathway activation. The most important genes driving the Wnt score were negative regulators of Wnt signaling (*ZNRF3*, *AXIN2*, and *NKD1*) (Fig 5A). The next highest-ranking gene was *ROR1*. Significantly, ROR1 (along with ROR2 and RYK) is a receptor for WNT5a and mediator of noncanonical Wnt signaling (32), suggesting that an important function for canonical Wnt/β-catenin signaling in PC may be to prime cells for responsiveness to noncanonical Wnt signaling (see below).

Further genes that were highly predictive of Wnt/β-catenin signaling were *AHR*, *DST*, *RAPH1*, and *MICAL2* (Fig. 5A). Aryl hydrocarbon receptor (AHR) has been implicated as a Wnt/β-catenin target gene in several cancers (33), and may play a role in maintaining stem cells (34). The latter three genes are involved in cell adhesion and migration. This analysis also identified *RUNX1* as a significant Wnt downstream effector in PC. One study indicated that RUNX1 contributes to PC growth (35), but it has not been linked to Wnt signaling. We confirmed Wnt regulation of AHR, ROR1, and RUNX1 by RT-qPCR (Fig. 5B) and immunoblotting (Fig. 5C).

As a further approach, we used a TCF-regulated luciferase reporter gene, which revealed substantial basal canonical Wnt signaling in R1 cells, a subline derived from CWR22 xenografts. Activity of the reporter gene and the expression of endogenous AXIN2 were markedly decreased by siRNA targeting WLS, indicating that it was driven by autocrine Wnt synthesis (Supplementary Fig. S7A). Notably, treatment with ETC-159 (PORCN inhibitor) suppressed the expression of ROR1, AHR and RUNX1 (Supplementary Fig. S7B). Finally, the growth of R1 xenografts was significantly suppressed by ETC-159 (Supplementary Fig. S7C), indicating that these tumors were dependent *in vivo* on autocrine Wnt synthesis.

Noncanonical Wnt signaling in mCRPC

The expression of WLS in mCRPC that is not strongly correlated with Wnt/β-catenin signaling suggested that Wnt synthesis may be preferentially driving noncanonical Wnt signaling in these cancers. However, an analysis of gene expression data in primary PC versus mCRPC did not reveal any clear alterations in relative expression of WNT5a or other Wnts (Supplementary Fig. S8A), or expression of Wnt receptors (Supplementary Fig. S8B). To further address the relationship between WLS expression and canonical Wnt/β-catenin signaling, we compared for all genes their correlation with WLS versus the Wnt activity score. There was a storng correlation in the TCGA primary PC dataset (Fig. 6A). In contrast, genes in the mCRPC datasets showed more divergence, with many genes being associated with WLS expression but not canonical Wnt/β-catenin signaling, consistent with WLS-dependent Wnt synthesis driving expression of additional noncanonical signaling pathways in mCRPC (Fig. 6A).

We then further interrogated clinical samples for genes associated with high Wnt activity. Among the top 1000 genes, 71 genes were shared in both primary PC and mCRPC (Supplementary Fig. S9A, B). Pathway analysis showed that no pathway other than Wnt signaling was represented in these 71 genes. *AXIN2*, *AHR*, *ROR1*, and *RUNX1* were included in these 71 genes, and they were more strongly correlated with WLS in the TCGA versus mCRPC datasets (Supplementary Table S5). Notably, we also found 46 genes commonly associated with high Wnt activity in mCRPC, but not in primary

PC (Supplementary Fig. S9C). These include genes related to the TGFβ pathway and *TNFRSF19* (previously described as a β-catenin target gene in human mesenchymal stem cells and prognostic marker in clinically localized PC for risk of metastatic progression) (36,37), which could represent canonical Wnt signaling functions related to metastasis or castration-resistance.

Conversely, we selected the top 1000 genes associated with WLS expression, but not the Wnt signature, in the mCRPC datasets. We identified 5 genes in common (*ERI3*, *HSDL1*, *CEACAM5*, *CEP41*, and *SCP2*) as potential targets of noncanonical Wnt signaling in mCRPC (Fig. 6B). *HSDL1* was reported to be increased in PC compared to normal prostate (38), but was also found to be highly methylated or have copy number loss in mCRPC (39). *CEACAM5* was reported as a tumor-associated surface antigen in neuroendocrine PC (40), and showed outlier levels of expression in neuroendocrine PC (41). To assess whether these five genes may be noncanonical Wnt effectors, we first surveyed WNT5a protein expression in PC cell lines to identify a model that may have basal autocrine noncanonical Wnt signaling, and found the highest level in LAPC4 cells (Fig. 6C). Stimulation of LAPC4 cells with WNT5a increased expression of all five genes, while *CEACAM5* and *ERI3* were induced by WNT5a in VCaP cells (Fig. 6D).

Previous studies have implicated canonical Wnt/β-catenin signaling in PC progression to mCRPC and resistance to ENZ or abiraterone (6–10,21,42), but have also found increased WNT5a and implicated increased noncanonical Wnt signaling (22,43). We addressed this further by assessing the canonical 47-gene WNT score in a set of CRPC patients stratified based on ENZ treatment (9). We did not find an increased WNT score in the ENZ-resistant versus naïve tumors, but did find WLS expression was elevated in the ENZ-resistant cases, with a trend toward increased CEACAM5 and CEP41 (Supplementary Fig. S10A). This analysis was also extended to scRNA-seq on a series of tumor biopsies from ENZ-exposed versus -naïve tumors (44). Both the 47-gene WNT score and WLS expression were heterogeneous in cells from the same biopsies, and consistent with the analysis of bulk sequencing in mCRPC, WLS expression was not correlated with the 47-gene WNT score (Fig. 6E). Moreover, the WNT score was not increased in cells from ENZ-exposed tumors (Fig. 6F). Finally, in one case where tumor biopsies were obtained before ENZ initiation and at progression, scRNA-seq showed an increase in WLS without an increase in the 47-gene WNT score (Supplementary Fig. S10B). Taken together these findings indicate that WNT synthesis is progressively skewed toward driving noncanonical signaling with progression to mCRPC and ENZ-resistance.

Canonical Wnt signaling primes for noncanonical signaling by increasing ROR1

We next carried out a matrix analysis of genes in the 47 gene Wnt signature to determine whether particular functions may predominate in some tumors. This identified clusters associated with noncanonical Wnt signaling (ROR1, KIF26b), metastasis (ODAM), a RUNX1 hub, and a stem cell hub headed by AHR and CD44 (Supplementary Fig. S11A). Notably, gene clusters comprised of canonical Wnt targets, including AXIN2, GPC4 and NKD1, may also interact with the noncanonical cluster represented by ROR1, KIF26b, the metastasis cluster (MICHEAL2 and ODAM), or with the AHR and CD44 stem hub.

The identification of a noncanonical Wnt signaling cluster including ROR1, a receptor for noncanonical Wnts, suggested that canonical WNT/β-catenin signaling may be priming for responsiveness to noncanonical Wnts. To test this hypothesis, we carried out APC knockdown in VCaP cells to increase the expression of ROR1, and then assessed responses to WNT5a. Indeed, after APC knockdown, cells became more responsive to WNT5a based on increased phosphorylation of Smad and CaMKII (Fig. 7A, B), which are downstream markers of noncanonical Wnt signaling (45). Moreover, the WNT5a treatment did not increase expression of AXIN2, KIF26b, or ROR1, indicating that it was not acting through canonical Wnt signaling (Fig. 7C).

To further assess whether ROR1 is directly regulated by Wnt/β-catenin in PC, we examined available *TCF7L2*/TCF4 ChIP-seq data in LNCaP cells, and in a CRC cell line with genomic Wnt/β-catenin pathway activation (HCT116 cells). Two TCF7L2 binding peaks were identified in both cell lines upstream of the ROR1 gene (Supplementary Fig. S11B). Notably, ChiP-seq showed an H3K27Ac peak overlapping the major TCF7L2 binding site in both VCaP and LNCaP PC cells, but not in two of three CRC lines. Together these findings support the conclusion that ROR1 is Wnt/β-catenin regulated in PC, but not consistently in CRC.

In vivo assessment of WNT dependence and the therapeutic effect of PORCN inhibition

We next examined a castration-resistant PDX (BIDPC5) generated from our rapid autopsy program (46). Immunohistochemistry revealed that WLS was highly expressed in multiple metastatic sites in this case (Fig. 7D) and in the PDX (Fig. 7E). Subcutaneous PDXs were generated and mice were then treated with vehicle, ENZ, or ETC-159 (47) for 3 weeks. Consistent with its castration-resistance, the PDX was not responsive to ENZ, while tumor growth was markedly suppressed by ETC-159 (Fig. 7F). Immunoblotting showed that LEF1, as well as ROR1, AHR, and RUNX1, were reduced in response to the PORCN inhibition, consistent with the latter genes being Wnt/β-catenin regulated in vivo (Fig. 7G).

To further assess Wnt dependence and the therapeutic effect of PORCN inhibition, we surveyed WLS expression by IHC in a series of LuCaP PDXs and identified two additional PDXs (LuCaP70CR and LuCaP77CR) with WLS expression (Supplementary Fig. S12A). Growth of LuCaP70CR, which expresses higher levels of WLS, was arrested by ETC-159 treatment (Supplementary Fig. S12B). LuCaP77CR PDXs were also suppressed by ETC-159, although this did not reach statistical significance.

DISCUSSION

Genomic alterations that activate Wnt/β-catenin signaling are relatively common in mCRPC (2–6), and activation of this pathway may drive resistance to AR-targeted therapies (6–10), but nongenomic activators of this pathway and its downstream effectors in PC remain to be established. We used WNT3a stimulation and APC depletion to identify downstream targets of Wnt/β-catenin signaling in a PC cell line, which were then integrated with clinical data to derive a 47-gene signature indicative of Wnt/β-catenin pathway activity in PC. Primary PC and mCRPC with genomic *APC* loss had comparable high Wnt scores based on this gene-set, but overall Wnt scores were lower in mCRPC, suggesting relatively lower activation

of this pathway by nongenomic mechanisms in CRPC. In addition to genomic alterations, *APC* expression may be decreased by methylation (11,12), but its decreased expression by this mechanism was not associated with increased Wnt score in clinical samples. Analysis for other potential upstream activators of Wnt signaling in primary PC identified *WLS*, which by IHC was found to be primarily expressed in tumor cells, indicating autocrine Wnt production as a driver of Wnt/β-catenin activity in primary PC. Notably, IHC showed that WLS was also highly expressed in the majority of mCRPC cases, but it was more weakly associated with the canonical WNT score, indicating that it may be more substantially driving noncanonical WNT signaling in mCRPC.

Consistent with noncanonical Wnt signaling in mCRPC, some previous studies have found increased expression of WNT5a in mCRPC (22,43). Notably, amongst the genes most highly associated with Wnt/β-catenin signaling was *ROR1*, a coreceptor for noncanonical Wnt signaling (32), indicating that one function of Wnt/β-catenin signaling in PC may be to prime tumor cells for noncanonical Wnt signaling. Indeed, we confirmed that increased ROR1 enhanced the response to WNT5a. Of note, while Wnt/β-catenin signaling is essential for prostate stem cell generation and proximal ductal outgrowth during prostate development, WNT5a and noncanonical Wnt signaling also play key roles in regulating these processes (48–50). We suggest this early Wnt/β-catenin developmental pathway, including priming for response to noncanonical Wnts, is reactivated in the microenvironment of primary PC.

AHR and *RUNX1* are two additional genes we found to be highly associated with Wnt/β-catenin signaling. AHR is most commonly associated with driving the metabolism of xenobiotic ligands, but also has context-dependent oncogenic and tumor-suppressive functions, the former including maintenance of cancer stem cells. One previous study found that it could be increased by β-catenin activation in some PC cell lines (33), while data from another group found that it was constitutively active and that its suppression by an inhibitor could decrease PC cell line growth (51). RUNX1 fusion proteins have been characterized as drivers of AML, but recent studies have established roles in the development of many tissues including prostate (52), and context-dependent oncogene or tumor-suppressor roles in several solid tumors. These findings indicate that AHR and RUNX1 are downstream effectors of Wnt/β-catenin signaling in PC that may contribute to oncogenic effects including stem cell maintenance and invasion.

Significantly, we confirmed that Wnt synthesis inhibition with a PORCN inhibitor *in vitro* and *in vivo* in PC models expressing WLS caused marked growth arrest and decreased expression of LEF1, AHR, RUNX1, and ROR1, consistent with suppression of Wnt/β-catenin signaling. While the decrease in ROR1 would also presumably suppress noncanonical Wnt signaling, its role in driving tumor growth is less clear. WNT5a signaling has been implicated in cancer cell invasion and metastasis, but it has also been reported to inhibit expansion of tumor-initiating cells and to induce PC dormancy (45,53). In any case, while suppression of Wnt/β-catenin and/or noncanonical Wnt signaling may be contributing to responses, we suggest that expression of WLS may be a biomarker of mCRPC that will respond to Wnt synthesis inhibition.

PC with genomic alterations upstream of the β-catenin destruction complex (*R-Spondin* gene fusions, loss of *RNF43* or *ZNRF3*) may also respond to agents including Wnt synthesis inhibitors or tankyrase inhibitors that stabilize the destruction complex. In contrast, the potential efficacy of these agents in tumors driven by alterations in *APC* is less clear. *APC* alterations in CRC are predominantly truncating mutations in the region that mediates β-catenin binding. Tumors with these truncating mutations may respond to tankyrase inhibitors, which is presumed to reflect some residual ability of the truncated APC (31). *APC* mutations in PC are similarly enriched for truncations in this region, and a subset may similarly respond to tankyrase inhibition. Surprisingly, a recent study in a GEM model of PC indicated that even tumors with biallelic loss of *APC* may respond to tankyrase inhibition, which presumably reflects some residual function of the destruction complex in the absence of APC (54). This could be a feature of PC that is distinct from CRC, as deep deletions of *APC* are rare in CRC, but appear more common in PC.

A further surprising finding was that epigenetic downregulation of APC was not associated with increased Wnt/β-catenin pathway activation, suggesting distinct tumor suppressor functions. Consistent with this hypothesis, while stable moderate downregulation of APC by shRNA only weakly increased Wnt/β-catenin pathway activity, it markedly enhanced xenograft establishment. Notably, amongst genes that are recurrently altered in PC, only *APC* alterations are enriched in metastatic versus primary castration-sensitive PC, indicating that these *APC* alterations confer metastatic potential rather than just resistance to AR-targeted therapies (4). Significantly, while alterations in *APC* may be oncogenic through several mechanisms, they may also create vulnerabilities that can be exploited therapeutically. However, further studies are needed to establish these additional oncogenic mechanisms and therapeutic vulnerabilities.

Previous studies have indicated that Wnt/β-catenin signaling is increased in mCRPC and may contribute to resistance to more intensive AR blockade (6–10), with one study finding that WLS was increased in PC cells treated with ENZ (55). While our data do not support a general increase in Wnt/β-catenin signaling in mCRPC, direct or indirect interactions with AR signaling are likely in a subset of tumors. Therefore, further studies into the efficacy of Wnt signaling inhibition, alone or in combination with AR targeted therapy, are warranted.

Supplementary Material

Refer to Web version on PubMed Central for supplementary material.

ACKNOWLEDGMENTS

This work was supported by NIH R01 CA168393 (XY, SPB), NIH P01 CA163227 (SPB), NIH P50 CA090381 (SPB, EVA), NIH T32 GM008313 (MXH), NSF grant GRFP DGE1144152 (MXH), Department of Defense PCRP Impact Award W81XWH-16-1-0431 (AGS, SPB), Department of Defense PCRP Idea Development Award W81XWH-20-1-0925 (FM, SPB), Department of Defense PCRP Idea Development Award W81XWH-15-1-0151 (XY), Prostate Cancer Foundation Challenge Award (SPB), Prostate Cancer Foundation Young Investigator Award (JWR), Bridge Project (partnership between the Koch Institute for Integrative Cancer Research at MIT and the Dana-Farber/Harvard Cancer Center) (SPB), JSPS Grant-in-Aid for Scientific Research (C) 20K09518 (SA), Research Fellowship from Gunma University Hospital (SA). We thank A*STAR (Singapore) for providing ETC-159.

REFERENCES

1. Cancer Genome Atlas Research N. The Molecular Taxonomy of Primary Prostate Cancer. Cell 2015;163(4):1011–25 doi 10.1016/j.cell.2015.10.025. [PubMed: 26544944]
2. Robinson D, Van Allen EM, Wu YM, Schultz N, Lonigro RJ, Mosquera JM, et al. Integrative clinical genomics of advanced prostate cancer. Cell 2015;161(5):1215–28 doi 10.1016/j.cell.2015.05.001. [PubMed: 26000489]
3. Kumar A, Coleman I, Morrissey C, Zhang X, True LD, Gulati R, et al. Substantial interindividual and limited intraindividual genomic diversity among tumors from men with metastatic prostate cancer. Nat Med 2016;22(4):369–78 doi 10.1038/nm.4053. [PubMed: 26928463]
4. Abida W, Armenia J, Gopalan A, Brennan R, Walsh M, Barron D, et al. Prospective Genomic Profiling of Prostate Cancer Across Disease States Reveals Germline and Somatic Alterations That May Affect Clinical Decision Making. JCO Precis Oncol 2017;2017 doi 10.1200/PO.17.00029.
5. Grasso CS, Wu YM, Robinson DR, Cao X, Dhanasekaran SM, Khan AP, et al. The mutational landscape of lethal castration-resistant prostate cancer. Nature 2012;487(7406):239–43 doi 10.1038/nature11125. [PubMed: 22722839]
6. Wang L, Dehm SM, Hillman DW, Sicotte H, Tan W, Gormley M, et al. A prospective genome-wide study of prostate cancer metastases reveals association of wnt pathway activation and increased cell cycle proliferation with primary resistance to abiraterone acetate-prednisone. Ann Oncol 2018;29(2):352–60 doi 10.1093/annonc/mdx689. [PubMed: 29069303]
7. Zhang Z, Cheng L, Li J, Farah E, Atallah NM, Pascuzzi PE, et al. Inhibition of the Wnt/beta-Catenin Pathway Overcomes Resistance to Enzalutamide in Castration-Resistant Prostate Cancer. Cancer Res 2018;78(12):3147–62 doi 10.1158/0008-5472.CAN-17-3006. [PubMed: 29700003]
8. Chen WS, Aggarwal R, Zhang L, Zhao SG, Thomas GV, Beer TM, et al. Genomic Drivers of Poor Prognosis and Enzalutamide Resistance in Metastatic Castration-resistant Prostate Cancer. Eur Urol 2019 doi 10.1016/j.eururo.2019.03.020.
9. Isaacsson Velho P, Fu W, Wang H, Mirkheshti N, Qazi F, Lima FAS, et al. Wnt-pathway Activating Mutations Are Associated with Resistance to First-line Abiraterone and Enzalutamide in Castration-resistant Prostate Cancer. Eur Urol 2020;77(1):14–21 doi 10.1016/j.eururo.2019.05.032. [PubMed: 31176623]
10. Wyatt AW, Azad AA, Volik SV, Annala M, Beja K, McConeghy B, et al. Genomic Alterations in Cell-Free DNA and Enzalutamide Resistance in Castration-Resistant Prostate Cancer. JAMA Oncol 2016;2(12):1598–606 doi 10.1001/jamaoncol.2016.0494. [PubMed: 27148695]
11. Yegnasubramanian S, Kowalski J, Gonzalgo ML, Zahurak M, Piantadosi S, Walsh PC, et al. Hypermethylation of CpG islands in primary and metastatic human prostate cancer. Cancer Res 2004;64(6):1975–86. [PubMed: 15026333]
12. Aryee MJ, Liu W, Engelmann JC, Nuhn P, Gurel M, Haffner MC, et al. DNA methylation alterations exhibit intraindividual stability and interindividual heterogeneity in prostate cancer metastases. Sci Transl Med 2013;5(169):169ra10 doi 10.1126/scitranslmed.3005211.
13. Wu L, Zhao JC, Kim J, Jin HJ, Wang CY, Yu J. ERG is a critical regulator of Wnt/LEF1 signaling in prostate cancer. Cancer Res 2013;73(19):6068–79 doi 10.1158/0008-5472.CAN-13-0882. [PubMed: 23913826]
14. Ma F, Ye H, He HH, Gerrin SJ, Chen S, Tanenbaum BA, et al. SOX9 drives WNT pathway activation in prostate cancer. J Clin Invest 2016;126(5):1745–58 doi 10.1172/JCI78815. [PubMed: 27043282]
15. Murillo-Garzon V, Kypta R. WNT signalling in prostate cancer. Nat Rev Urol 2017;14(11):683–96 doi 10.1038/nrurol.2017.144. [PubMed: 28895566]
16. Yu X, Wang Y, Jiang M, Bierie B, Roy-Burman P, Shen MM, et al. Activation of beta-Catenin in mouse prostate causes HGPIN and continuous prostate growth after castration. Prostate 2009;69(3):249–62 doi 10.1002/pros.20877. [PubMed: 18991257]
17. Bierie B, Nozawa M, Renou JP, Shillingford JM, Morgan F, Oka T, et al. Activation of beta-catenin in prostate epithelium induces hyperplasias and squamous transdifferentiation. Oncogene 2003;22(25):3875–87 doi 10.1038/sj.onc.1206426. [PubMed: 12813461]

18. Gounari F, Signoretti S, Bronson R, Klein L, Sellers WR, Kum J, et al. Stabilization of beta-catenin induces lesions reminiscent of prostatic intraepithelial neoplasia, but terminal squamous transdifferentiation of other secretory epithelia. Oncogene 2002;21(26):4099–107 doi 10.1038/sj.onc.1205562. [PubMed: 12037666]

19. Francis JC, Thomsen MK, Taketo MM, Swain A. beta-catenin is required for prostate development and cooperates with Pten loss to drive invasive carcinoma. PLoS Genet 2013;9(1):e1003180 doi 10.1371/journal.pgen.1003180. [PubMed: 23300485]

20. Bruxvoort KJ, Charbonneau HM, Giambernardi TA, Goolsby JC, Qian CN, Zylstra CR, et al. Inactivation of Apc in the mouse prostate causes prostate carcinoma. Cancer Res 2007;67(6):2490–6 doi 10.1158/0008-5472.CAN-06-3028. [PubMed: 17363566]

21. Schneider JA, Logan SK. Revisiting the role of Wnt/beta-catenin signaling in prostate cancer. Mol Cell Endocrinol 2018;462(Pt A):3–8 doi 10.1016/j.mce.2017.02.008. [PubMed: 28189566]

22. Miyamoto DT, Zheng Y, Wittner BS, Lee RJ, Zhu H, Broderick KT, et al. RNA-Seq of single prostate CTCs implicates noncanonical Wnt signaling in antiandrogen resistance. Science 2015;349(6254):1351–6 doi 10.1126/science.aab0917. [PubMed: 26383955]

23. Sun Y, Campisi J, Higano C, Beer TM, Porter P, Coleman I, et al. Treatment-induced damage to the tumor microenvironment promotes prostate cancer therapy resistance through WNT16B. Nat Med 2012;18(9):1359–68 doi 10.1038/nm.2890. [PubMed: 22863786]

24. Verhaegh W, van Ooijen H, Inda MA, Hatzis P, Versteeg R, Smid M, et al. Selection of personalized patient therapy through the use of knowledge-based computational models that identify tumor-driving signal transduction pathways. Cancer Res 2014;74(11):2936–45 doi 10.1158/0008-5472.CAN-13-2515. [PubMed: 24695361]

25. Gregory CW, Whang YE, McCall W, Fei X, Liu Y, Ponguta LA, et al. Heregulin-induced activation of HER2 and HER3 increases androgen receptor transactivation and CWR-R1 human recurrent prostate cancer cell growth. Clin Cancer Res 2005;11(5):1704–12 doi 10.1158/1078-0432.CCR-04-1158. [PubMed: 15755991]

26. Shourideh M, DePriest A, Mohler JL, Wilson EM, Koochekpour S. Characterization of fibroblast-free CWR-R1ca castration-recurrent prostate cancer cell line. Prostate 2016;76(12):1067–77 doi 10.1002/pros.23190. [PubMed: 27271795]

27. Hankey W, Frankel WL, Groden J. Functions of the APC tumor suppressor protein dependent and independent of canonical WNT signaling: implications for therapeutic targeting. Cancer Metastasis Rev 2018;37(1):159–72 doi 10.1007/s10555-017-9725-6. [PubMed: 29318445]

28. Zhang L, Shay JW. Multiple Roles of APC and its Therapeutic Implications in Colorectal Cancer. J Natl Cancer Inst 2017;109(8) doi 10.1093/jnci/djw332.

29. Niehrs C, Acebron SP. Mitotic and mitogenic Wnt signalling. EMBO J 2012;31(12):2705–13 doi 10.1038/emboj.2012.124. [PubMed: 22617425]

30. Quigley DA, Dang HX, Zhao SG, Lloyd P, Aggarwal R, Alumkal JJ, et al. Genomic Hallmarks and Structural Variation in Metastatic Prostate Cancer. Cell 2018;174(3):758–69 e9 doi 10.1016/j.cell.2018.06.039. [PubMed: 30033370]

31. Schatoff EM, Goswami S, Zafra MP, Foronda M, Shusterman M, Leach BI, et al. Distinct Colorectal Cancer-Associated APC Mutations Dictate Response to Tankyrase Inhibition. Cancer Discov 2019;9(10):1358–71 doi 10.1158/2159-8290.CD-19-0289. [PubMed: 31337618]

32. Roy JP, Halford MM, Stacker SA. The biochemistry, signalling and disease relevance of RYK and other WNT-binding receptor tyrosine kinases. Growth Factors 2018;36(1–2):15–40 doi 10.1080/08977194.2018.1472089. [PubMed: 29806777]

33. Chesire DR, Dunn TA, Ewing CM, Luo J, Isaacs WB. Identification of aryl hydrocarbon receptor as a putative Wnt/beta-catenin pathway target gene in prostate cancer cells. Cancer Res 2004;64(7):2523–33. [PubMed: 15059908]

34. Stanford EA, Wang Z, Novikov O, Mulas F, Landesman-Bollag E, Monti S, et al. The role of the aryl hydrocarbon receptor in the development of cells with the molecular and functional characteristics of cancer stem-like cells. BMC Biol 2016;14:20 doi 10.1186/s12915-016-0240-y. [PubMed: 26984638]

35. Takayama K, Suzuki T, Tsutsumi S, Fujimura T, Urano T, Takahashi S, et al. RUNX1, an androgen- and EZH2-regulated gene, has differential roles in AR-dependent and -independent

prostate cancer. Oncotarget 2015;6(4):2263–76 doi 10.18632/oncotarget.2949. [PubMed: 25537508]

36. Qiu W, Hu Y, Andersen TE, Jafari A, Li N, Chen W, et al. Tumor necrosis factor receptor superfamily member 19 (TNFRSF19) regulates differentiation fate of human mesenchymal (stromal) stem cells through canonical Wnt signaling and C/EBP. J Biol Chem 2010;285(19):14438–49 doi 10.1074/jbc.M109.052001. [PubMed: 20223822]
37. Rubicz R, Zhao S, Wright JL, Coleman I, Grasso C, Geybels MS, et al. Gene expression panel predicts metastatic-lethal prostate cancer outcomes in men diagnosed with clinically localized prostate cancer. Mol Oncol 2017;11(2):140–50 doi 10.1002/1878-0261.12014. [PubMed: 28145099]
38. Huang Y, Tang R, Dai J, Gu S, Zhao W, Cheng C, et al. A novel human hydroxysteroid dehydrogenase like 1 gene (HSDL1) is highly expressed in reproductive tissues. Mol Biol Rep 2001;28(4):185–91 doi 10.1023/a:1015726217890. [PubMed: 12153137]
39. Friedlander TW, Roy R, Tomlins SA, Ngo VT, Kobayashi Y, Azameera A, et al. Common structural and epigenetic changes in the genome of castration-resistant prostate cancer. Cancer Res 2012;72(3):616–25 doi 10.1158/0008-5472.CAN-11-2079. [PubMed: 22158653]
40. Lee JK, Bangayan NJ, Chai T, Smith BA, Pariva TE, Yun S, et al. Systemic surfaceome profiling identifies target antigens for immune-based therapy in subtypes of advanced prostate cancer. Proc Natl Acad Sci U S A 2018;115(19):E4473–E82 doi 10.1073/pnas.1802354115. [PubMed: 29686080]
41. Beltran H, Prandi D, Mosquera JM, Benelli M, Puca L, Cyrta J, et al. Divergent clonal evolution of castration-resistant neuroendocrine prostate cancer. Nat Med 2016;22(3):298–305 doi 10.1038/nm.4045. [PubMed: 26855148]
42. Patel R, Brzezinska EA, Repiscak P, Ahmad I, Mui E, Gao M, et al. Activation of beta-Catenin Cooperates with Loss of Pten to Drive AR-Independent Castration-Resistant Prostate Cancer. Cancer Res 2020;80(3):576–90 doi 10.1158/0008-5472.CAN-19-1684. [PubMed: 31719098]
43. Stanbrough M, Bubley GJ, Ross K, Golub TR, Rubin MA, Penning TM, et al. Increased expression of genes converting adrenal androgens to testosterone in androgen-independent prostate cancer. Cancer Res 2006;66(5):2815–25 doi 10.1158/0008-5472.CAN-05-4000. [PubMed: 16510604]
44. He MX, Cuoco MS, Crowdis J, Bosma-Moody A, Zhang Z, Bi K, et al. Transcriptional mediators of treatment resistance in lethal prostate cancer. Nat Med 2021;27(3):426–33 doi 10.1038/s41591-021-01244-6. [PubMed: 33664492]
45. Borcherding N, Kusner D, Kolb R, Xie Q, Li W, Yuan F, et al. Paracrine WNT5A Signaling Inhibits Expansion of Tumor-Initiating Cells. Cancer Res 2015;75(10):1972–82 doi 10.1158/0008-5472.CAN-14-2761. [PubMed: 25769722]
46. Einstein DJ, Arai S, Calagua C, Xie F, Voznesensky O, Capaldo BJ, et al. Metastatic Castration-Resistant Prostate Cancer Remains Dependent on Oncogenic Drivers Found in Primary Tumors. JCO Precis Oncol 2021;5 doi 10.1200/PO.21.00059.
47. Madan B, Ke Z, Harmston N, Ho SY, Frois AO, Alam J, et al. Wnt addiction of genetically defined cancers reversed by PORCN inhibition. Oncogene 2016;35(17):2197–207 doi 10.1038/onc.2015.280. [PubMed: 26257057]
48. Huang L, Pu Y, Hu WY, Birch L, Luccio-Camelo D, Yamaguchi T, et al. The role of Wnt5a in prostate gland development. Dev Biol 2009;328(2):188–99 doi 10.1016/j.ydbio.2009.01.003. [PubMed: 19389372]
49. Simons BW, Hurley PJ, Huang Z, Ross AE, Miller R, Marchionni L, et al. Wnt signaling though beta-catenin is required for prostate lineage specification. Dev Biol 2012;371(2):246–55 doi 10.1016/j.ydbio.2012.08.016. [PubMed: 22960283]
50. Wei X, Zhang L, Zhou Z, Kwon OJ, Zhang Y, Nguyen H, et al. Spatially Restricted Stromal Wnt Signaling Restrains Prostate Epithelial Progenitor Growth through Direct and Indirect Mechanisms. Cell Stem Cell 2019;24(5):753–68 e6 doi 10.1016/j.stem.2019.03.010. [PubMed: 30982770]
51. Richmond O, Ghotbaddini M, Allen C, Walker A, Zahir S, Powell JB. The aryl hydrocarbon receptor is constitutively active in advanced prostate cancer cells. PLoS One 2014;9(4):e95058 doi 10.1371/journal.pone.0095058. [PubMed: 24755659]

52. Mevel R, Steiner I, Mason S, Galbraith LC, Patel R, Fadlullah MZ, et al. RUNX1 marks a luminal castration-resistant lineage established at the onset of prostate development. Elife 2020;9 doi 10.7554/eLife.60225.

53. Ren D, Dai Y, Yang Q, Zhang X, Guo W, Ye L, et al. Wnt5a induces and maintains prostate cancer cells dormancy in bone. J Exp Med 2019;216(2):428–49 doi 10.1084/jem.20180661. [PubMed: 30593464]

54. Leibold J, Ruscetti M, Cao Z, Ho YJ, Baslan T, Zou M, et al. Somatic Tissue Engineering in Mouse Models Reveals an Actionable Role for WNT Pathway Alterations in Prostate Cancer Metastasis. Cancer Discov 2020;10(7):1038–57 doi 10.1158/2159-8290.CD-19-1242. [PubMed: 32376773]

55. Lombard AP, Liu C, Armstrong CM, D'Abronzo LS, Lou W, Evans CP, et al. Wntless promotes cellular viability and resistance to enzalutamide in castration-resistant prostate cancer cells. Am J Clin Exp Urol 2019;7(4):203–14. [PubMed: 31511827]

Significance Statement

This work provides fundamental insights into Wnt signaling and prostate cancer cell biology and indicate that a subset of prostate cancer driven by autocrine Wnt signaling is sensitive to Wnt synthesis inhibitors.

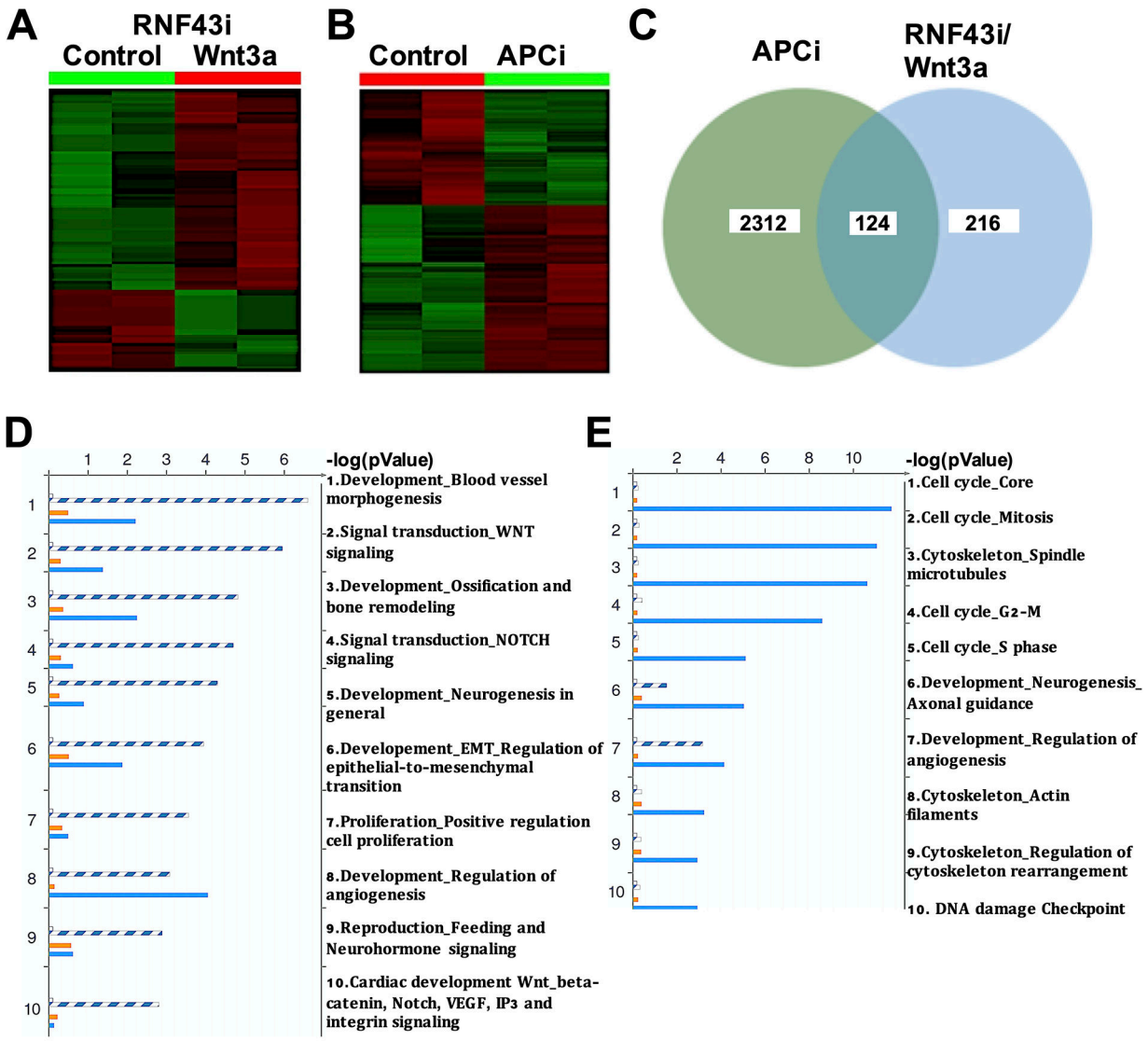

Figure 1. Transcriptome profiling of canonical Wnt/β-catenin signaling in PC cells.

A, Differentially expressed genes between VCaP with (n=2) or without (n=2) WNT3a/RNF43 knockdown (p-value <0.05). **B**, Differentially expressed genes between VCaP with control siRNA (n=2) and APC siRNA (n=2) (p-value <0.05). **C**, Overlap of differentially expressed genes from the two treatments. **D**, Enriched pathways based on shared genes. **E**, Enriched pathways for genes regulated only by APC. Enrichment was by Metacore Pathway Enrichment Analysis, p<0.01. Blue stripes, enrichment for the common 124 genes; Orange solid bars, enrichment for genes uniquely regulated with RNF43i/WNT3a; blue solid bars, enrichment for genes uniquely regulated upon APC knockdown.

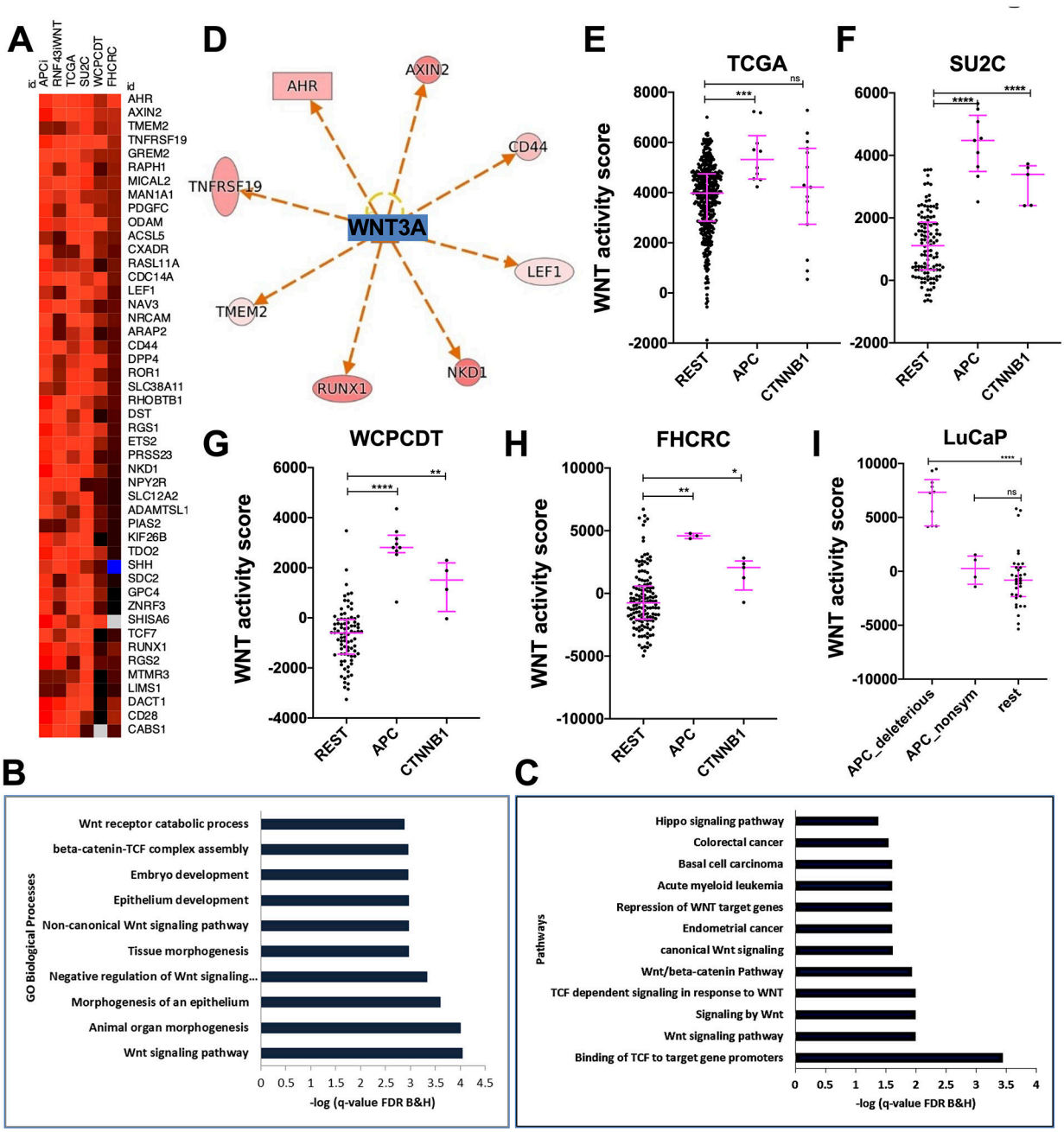

Figure 2. Wnt signature derived by integrative analysis of VCaP cells and clinical datasets predicts Wnt activities.

A, Fold change of 47-geneset between Wnt-high versus Wnt-low status in clinical datasets and VCaP with APC knockdown (APCi) and WNT3a/RNF43 knockdown. Patients were stratified into Wnt-high (WH, top 10% Wnt activity score based on 124 gene set) and Wnt-low (WL, bottom 10% of the Wnt activity score) within TCGA (WH, n=55 vs WL, n=105), SU2C (WH, n=14 vs WL, n=14), WCPCDT (WH, n=14 vs WL, n=11) and FHCRC (WH, n=28 vs WL, n=16) datasets. **B**, **C**, GO biological processes or Pathway enrichment for 47-geneset with P value <0.01. **D**, Upstream prediction analysis. **E-I**, Scatter plots, with lines at median and interquartile ranges, show Wnt activity score distributions

in cases with or without *APC*/*CTNNB1* alterations in the following clinical datasets and one PDX dataset: **E**, TCGA (Rest, n=449; *APC*, n=10; *CTNNB1*, n=15); **F**, SU2C (Rest, n=118; APC, n=9, CTNNB1, n=4); **G**, WCPCDT (Rest, n=141; *APC*, n=3; *CTNNB1*, n=5); **H**, FHCRC (Rest, n=141; *APC*, n=3; *CTNNB1*, n=5); **I**, LuCaP PDX series (Rest, n=34; APC-deleterious stands for *APC* loss/truncation mutations, n=10; *APC*-nonsym is nonsynonymous mutations of unclear functional significance, n=4). Mann-Whitney tests, cutoff $p<0.05$. **** = $p<0.0001$, *** = $p<0.001$, ** = $p<0.01$, * = $p<0.05$, ns = no significance.

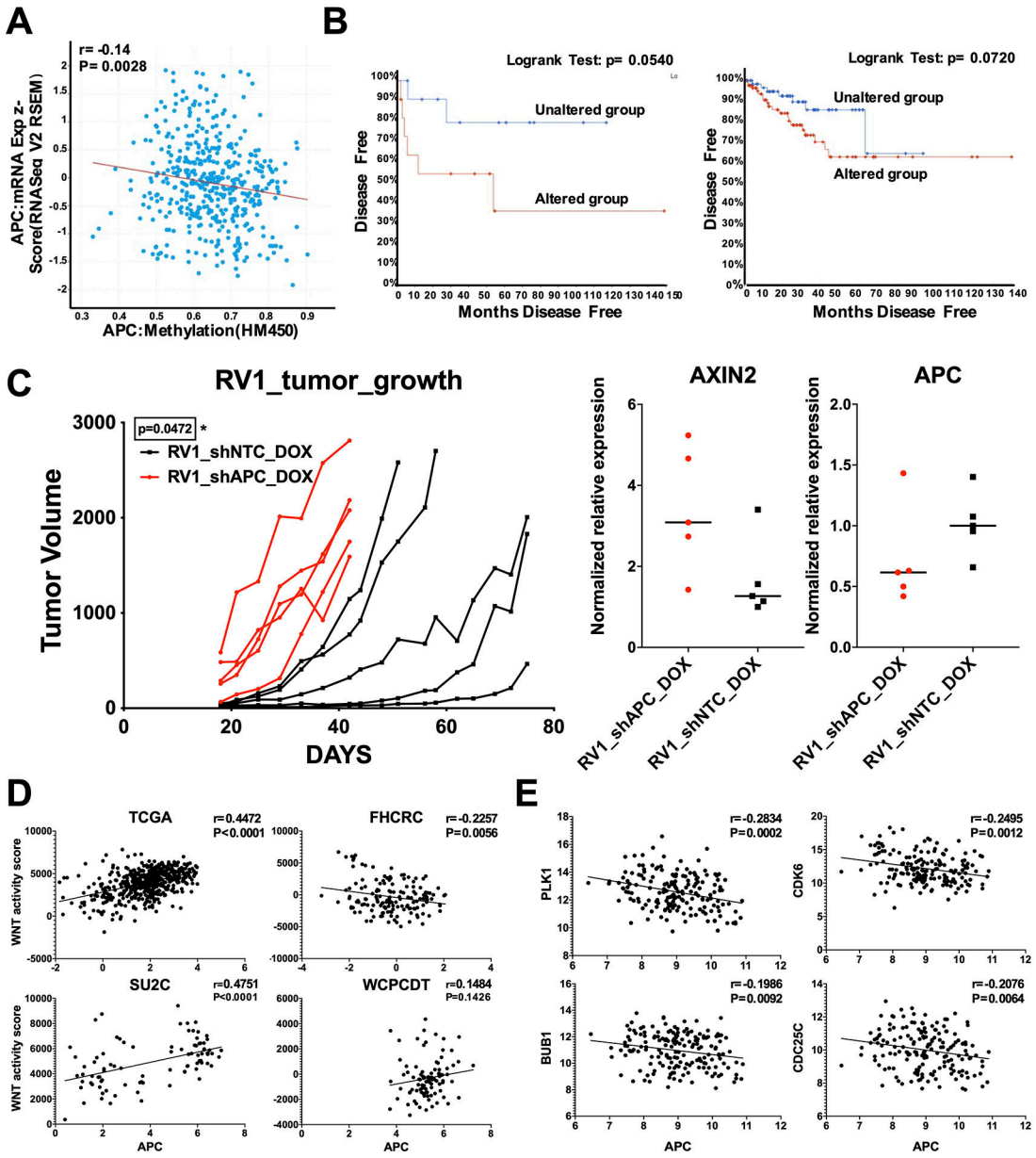

Figure 3. Epigenetic downregulation of APC promotes tumor growth but does not correlate with Wnt/β-catenin pathway activation.

A, Expression correlation analysis of *APC* with promoter methylation in TCGA (n=436, cases with genomic *APC* alterations excluded). **B**, Kaplan Meier survival analysis of cases with different APC expression levels in MSKCC (Memorial Sloan Kettering Cancer Center) and TCGA datasets. Left panel: MSKCC (Unaltered group represents APC expression z>0.7, n=12; Altered group represents APC expression z<−1.7, n=11). Right panel: TCGA (Unaltered group represents APC expression z>0.7, n=62; Altered group represents APC expression z<−0.7, n=86). Statistics: Log-rank Test performed. **C**, Left panel: Growth curves of xenografts derived from RV1 cells with either doxycycline-inducible shAPC (RV1_shAPC_DOX, red curves) or shNTC (non-target control, RV1_shNTC_DOX, black curves). Middle and right panels: qRT-PCR for APC (middle panel) or AXIN2 (right panel)

in RV1_shAPC_DOX (red dots) and RV1_shNTC_DOX (black dots) harvested at indicated endpoints. **D**, Expression correlation of APC with WNT activity scores in TCGA (n=548), FHCRC (n=149), SU2C (n=89) and WCPCDT (n=99) datasets. **E**, Expression correlation of APC with cell cycle genes *PLK1*, *BUB1*, *CDK6* and *CDC25C* in FHCRC (n=149) dataset. A, D and E statistics: Pearson correlation and linear regression. C statistics: Mann-Whitney test. $P<0.05$ deemed significant.

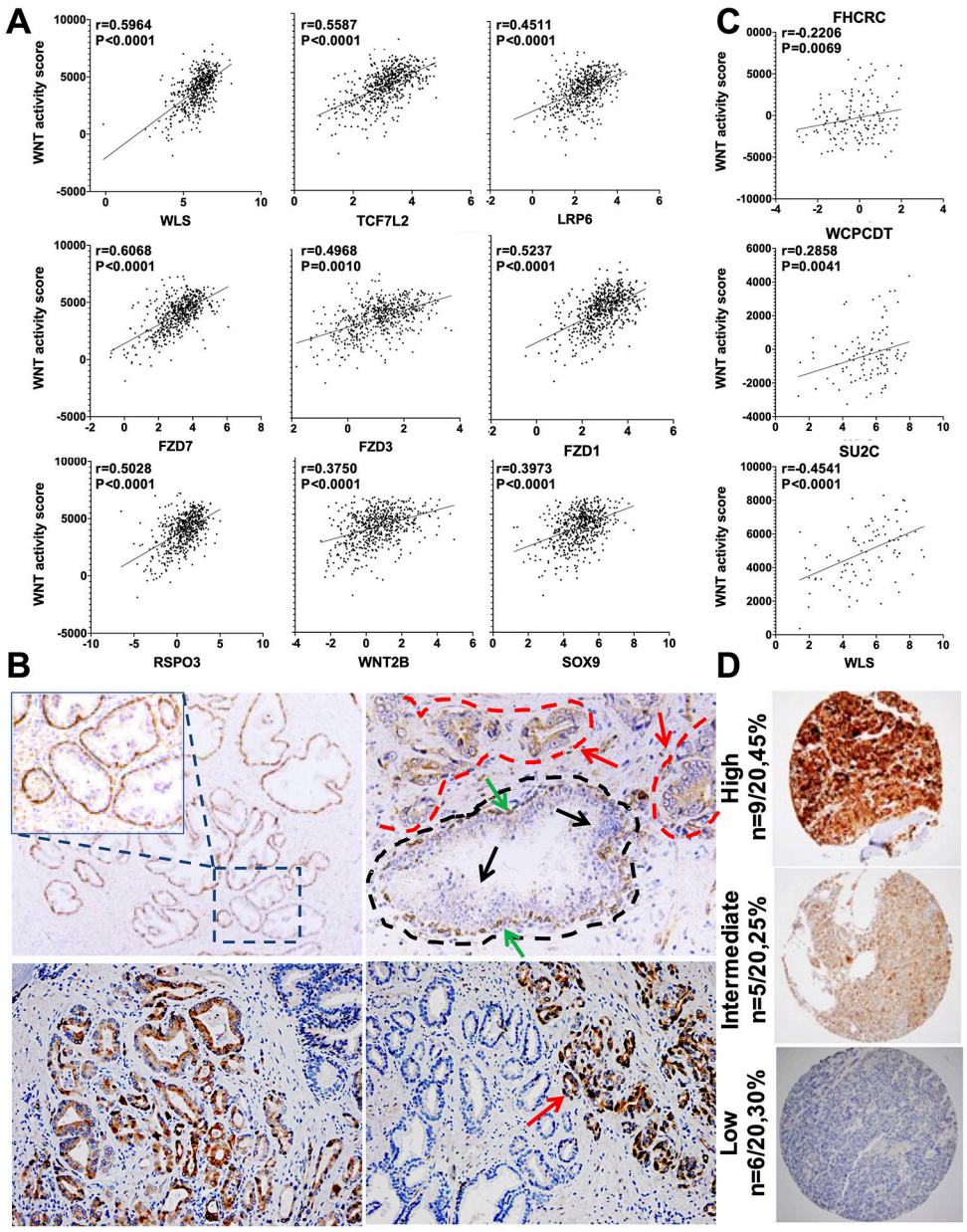

Figure 4. Wnt/β-catenin activity is correlated with tumor cell expression of WLS.

A, Expression correlation between potential Wnt drivers and WNT activity in TCGA (n=448) dataset. **B**, Representative IHC of WLS in prostate. Upper left, normal prostate glands with magnified focus area. Upper right, PIN lesions (black dashed line circles a PIN focus, black arrows indicate luminal tumor cells; green arrows indicate basal cells; red circles and arrows indicate surrounding tumor foci and lack ok basal cells). Lower panels show WLS in primary PC, with heterogeneous WLS expression shown in lower right (tumor area with positive WLS staining indicated by a red arrow). **C**, Correlation between WLS mRNA and Wnt activity in FHCRC (n=149), WCPCDT (n=99) and SU2C (n=89) datasets. **D**, Representative IHC of WLS in a TMA of mCRPC (n=20), showing a range from negative

to strong staining patterns. A and C statistics: Pearson correlations with linear regression, correlation scores (r) and p values are shown. Significant: $P<0.05$.

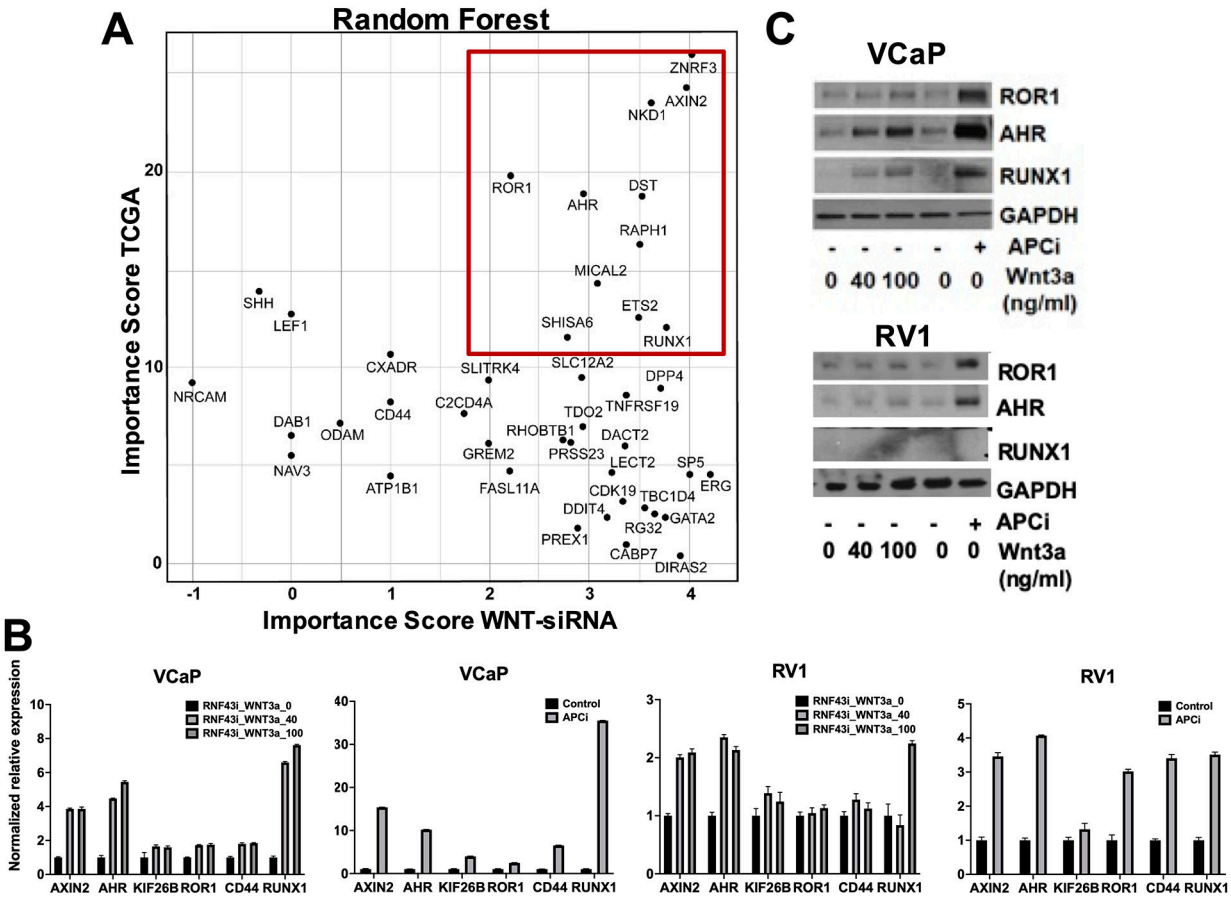

Figure 5. Downstream effectors of canonical Wnt/β-catenin signaling in PC.

A, Random forest analysis intersecting genes most correlated with Wnt/β-catenin pathway activation in TCGA dataset and in VCaP cells with APC knockdown and RNF43i/WNT3a stimulation. **B**, qRT-PCR for downstream effectors of Wnt/β-catenin signaling in VCaP and RV1 cells with RNF43i/WNT3a stimulation (40 or 100 ng/ml) or APC knockdown. **C**, Immunoblotting of Wnt/β-catenin targets in VCaP (left panel) and RV1 (right panel) after RNF43i/WNT3a stimulation or APC knockdown (representative of at least 3 replicates).

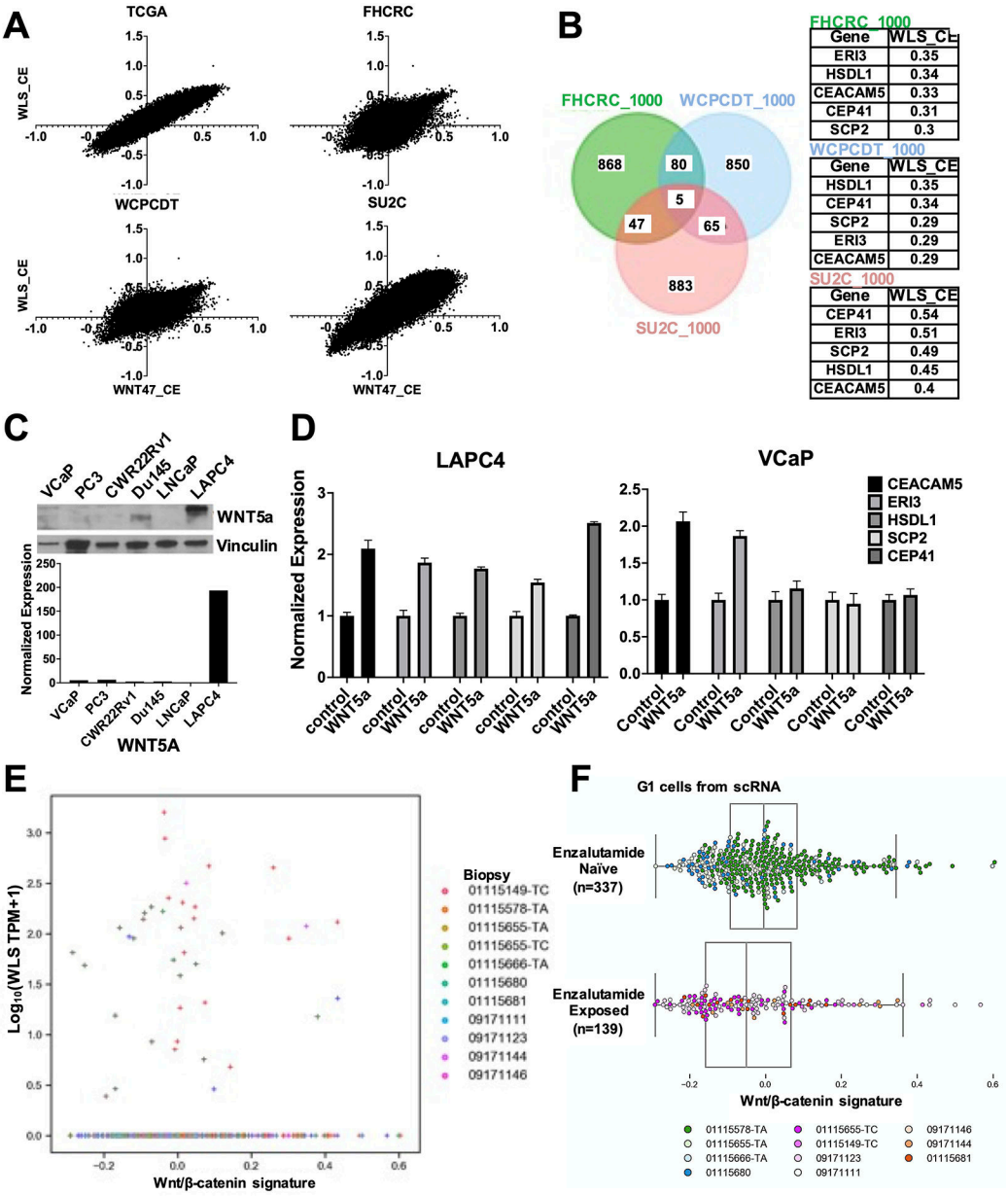

Figure 6. WLS association with canonical versus noncanonical Wnt signaling in mCRPC.

A, Plot comparing for all genes their correlation with WLS expression versus WNT47 signature using the corresponding correlation coefficients (WLS_CE and WNT47_CE). The correlations were assessed for TCGA, FHCRC, WCPCDT and SU2C datasets. **B**, Left panel, overlap of the top thousand genes correlating with WLS expression and not the WNT47 signature in mCRPC datasets: FHCRC, WCPCDT and SU2C. Right panel, common five potential noncanonical effectors and their corresponding correlation coefficients with WLS. **C**, WNT5A across a panel of PC cell lines by both RT-qPCR and immunoblotting. **D**, RT-qPCR quantification of the five potential noncanonical effectors in response to WNT5a stimulation in LAPC4 and VCaP. **E**, Distribution of WLS from scRNA-seq analysis of mCRPC tumor biopsies and its association with Wnt activity defined by WNT47 signature.

F, Scatter plots with lines at median and interquartile ranges of Wnt activity between ENZ-naïve (n=337) and ENZ-exposed (n=139) cells from scRNA-seq dataset.

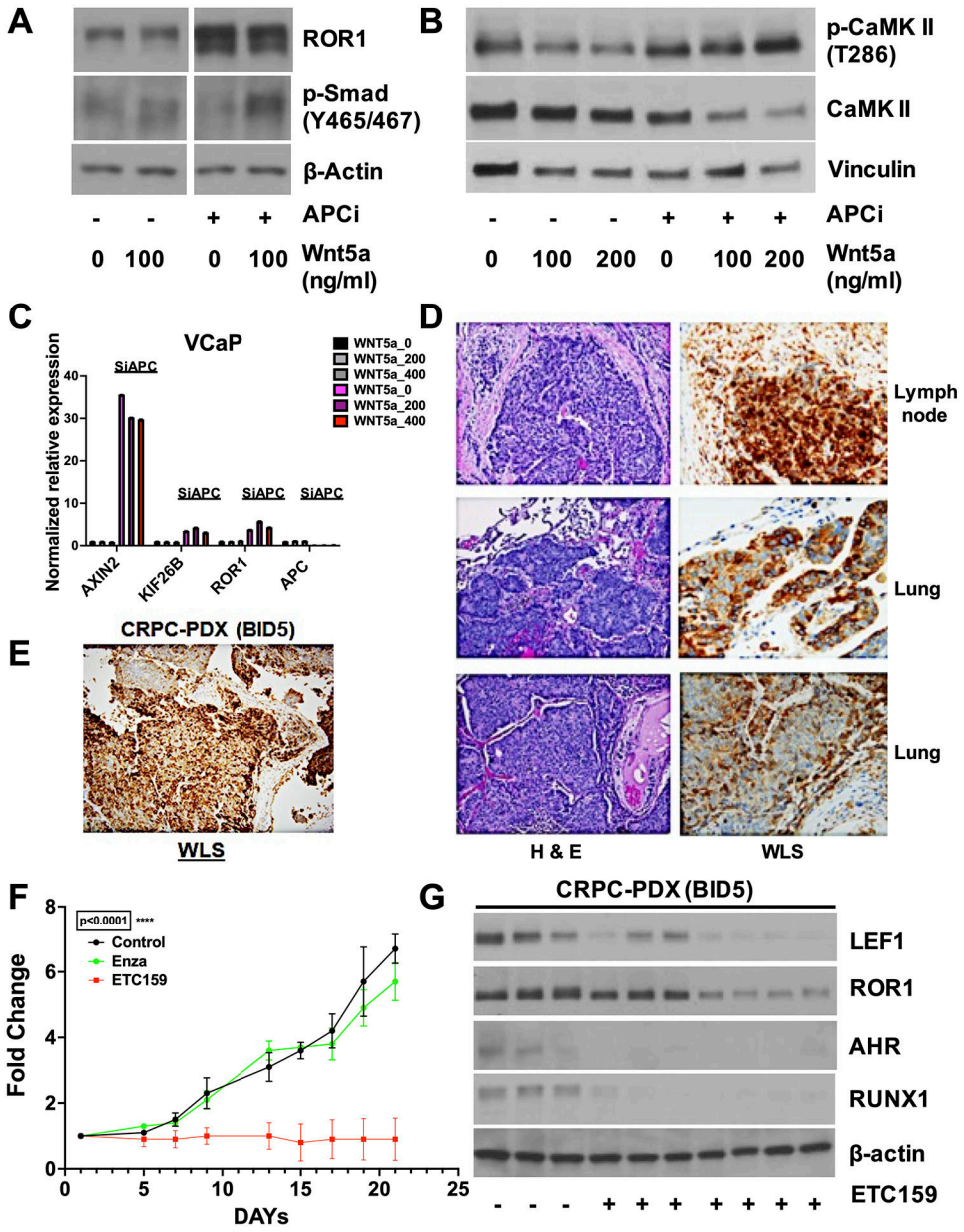

Figure 7. WNT/β-catenin signaling increases ROR1 in vivo and primes for noncanonical Wnt signaling.

A-C, VCaP cells were treated with control or APC siRNA for 3 days followed by stimulation with WNT5a for 6 hours and immunoblotting or qRT-PCR. **A** and **B**, show p-Smad and p-CAMKII responses to WNT5a with increased ROR1 (representative of at least 3 replicates). **C**, qRT-PCR confirming APC depletion and showing that WNT5a is not increasing canonical Wnt/β-catenin target genes. **D**, Representative images of H&E and WLS IHC from multiple metastatic sites in ENZ-resistant rapid autopsy case. **E**, Representative image of WLS IHC from PDX BIDPC5 (BID5) generated from the case in (D). **F**, Growth curves of PDX treated with vehicle (black, n=3), ENZ (green, n=3), or ETC-159 (red, n=9). Statistics: Mann-Whitney test compared the difference between the

ETC-159 and control arms. **G**, WNT/β-catenin effectors in response to PORCN inhibition compared with untreated controls from tumors collected at the treatment endpoints.